Targeting Plasma Kallikrein With a Novel Bicyclic Peptide Inhibitor (THR-149) Reduces Retinal Thickening in a Diabetic Rat Model

Tine Van Bergen,[1] Tjing-Tjing Hu,[1] Karis Little,[2] Lies De Groef,[3] Lieve Moons,[3] Alan W. Stitt,[1,2] Elke Vermassen,[1] and Jean H. M. Feyen[1]

[1]Oxurion NV, Heverlee, Belgium
[2]Queen's University Belfast, Belfast, United Kingdom
[3]Neural Circuit Development and Regeneration Research Group, Department of Biology and Leuven Brain Institute, KU Leuven, Leuven, Belgium

Correspondence: Tine Van Bergen, Oxurion NV, Gaston Geenslaan 1, B-3001, Heverlee, Belgium; tine.vanbergen@oxurion.com.

Received: November 30, 2020
Accepted: August 27, 2021
Published: October 22, 2021

Citation: Van Bergen T, Hu TT, Little K, et al. Targeting plasma kallikrein with a novel bicyclic peptide inhibitor (THR-149) reduces retinal thickening in a diabetic rat model. *Invest Ophthalmol Vis Sci.* 2021;62(13):18. https://doi.org/10.1167/iovs.62.13.18

Purpose. To investigate the effect of plasma kallikrein (PKal)-inhibition by THR-149 on preventing key pathologies associated with diabetic macular edema (DME) in a rat model.

Methods. Following streptozotocin-induced diabetes, THR-149 or its vehicle was administered in the rat via either a single intravitreal injection or three consecutive intravitreal injections (with a 1-week interval; both, 12.5 µg/eye). At 4 weeks post-diabetes, the effect of all groups was compared by histological analysis of Iba1-positive retinal inflammatory cells, inflammatory cytokines, vimentin-positive Müller cells, inwardly rectifying potassium and water homeostasis-related channels (Kir4.1 and AQP4, respectively), vascular leakage (fluorescein isothiocyanate-labeled bovine serum albumin), and retinal thickness.

Results. Single or repeated THR-149 injections resulted in reduced inflammation, as depicted by decreasing numbers and activation state of immune cells and IL-6 cytokine levels in the diabetic retina. The processes of reactive gliosis, vessel leakage, and retinal thickening were only significantly reduced after multiple THR-149 administrations. Individual retinal layer analysis showed that repeated THR-149 injections significantly decreased diabetes-induced thickening of the inner plexiform, inner nuclear, outer nuclear, and photoreceptor layers. At the glial–vascular interface, reduced Kir4.1-channel levels in the diabetic retina were restored to control non-diabetic levels in the presence of THR-149. In contrast, little or no effect of THR-149 was observed on the AQP4-channel levels.

Conclusions. These data demonstrate that repeated THR-149 administration reduces several DME-related key pathologies such as retinal thickening and neuropil disruption in the diabetic rat. These observations indicate that modulation of the PKal pathway using THR-149 has clinical potential to treat patients with DME.

Keywords: plasma kallikrein, diabetic macular edema, retinal thickening, inflammation, gliosis

Diabetic retinopathy (DR) is a leading cause of visual impairment in the working-age population and is one of the most common complications of diabetes mellitus.[1] The exact pathogenic mechanisms involved in DR remain elusive, although it is thought that hyperglycemia and other components of the complex diabetic milieu lead to activation of pathways such as oxidative stress and inflammation that have been linked to glial activation in unison with neuronal and vascular cell dysfunction and death. Vascular dysfunction and inflammation, leading to microvascular retinal damage such as microaneurysms, capillary drop-out, and ischemia, can eventually result in overt blood–retinal barrier (BRB) breakdown and impaired fluid homeostasis (diabetic macular edema [DME]) and/or abnormal growth of new blood vessels (proliferative diabetic retinopathy), causing moderate to severe vision loss.[2,3] The gold-standard treatment for DME is intravitreal (IVT) injections of anti-vascular endothelial growth factor (VEGF) agents although panretinal laser photocoagulation and steroids are also used.[4] Importantly, not all patients respond optimally to anti-VEGF therapy,[5,6] and there is a pressing need for alternative therapies that can reverse DME.

Plasma kallikrein (PKal) has been identified as a potential target for the treatment of DME.[7–9] PKal is a serine protease positioned at the interface between the contact activation system and the kallikrein–kinin system (KKS). Within the KKS, PKal activity releases bradykinin (BK) from the high-molecular-weight kininogen. BK then signals through the bradykinin B2 receptor (B2R) and, via its des-Arg9 metabolite, through the inducible bradykinin B1 receptor (B1R), leading to the production of mediators of inflammation, angiogenesis, vasodilation, and increased vessel

permeability.[9] Levels of PKal and other components of the KKS are described to be higher in diabetic animal models,[10,11] as well as in the vitreous fluid of DME patients.[12–14] Moreover, administration of PKal and BK has been demonstrated to increase vascular permeability and retinal thickness in wild-type and diabetic animals,[12,15,16] whereas inhibition or deficiency of PKal or B1/B2 receptors improved BRB integrity by reducing the leukocyte cell number, the level of proinflammatory cytokines, vascular permeability, retinal thickening, and oxidative stress in diabetic animal models.[17–20]

A library of bicyclic peptide PKal inhibitor analogs was generated[21] from which a potent and stable inhibitor was selected. Named THR-149, this agent was shown to prevent diabetes-induced retinal leakage in a diabetic rat model (Van Bergen T et al.[68]). Building on this foundation evidence, the aim of the current study was to confirm these data and to evaluate the impact of PKal inhibition on diabetes-induced retinal thickening. Moreover, to unravel the mechanism of THR-149, a range of inter-related key pathologies with relevance to DME was checked, such as (re)activation of retinal inflammatory and Müller cells, as well as its effect on proinflammatory cytokines, on inwardly rectifying potassium (Kir) channel subunit Kir4.1, and on the water channel aquaporin 4 (AQP4). These channels are known to be involved in retinal edema, and expression has been reported to be changed in the diabetic rat retina.[22]

Methods

All experimental animal procedures were approved by the Institutional Animal Care and Research Advisory Committee of the KU Leuven, according to the 2010/63/EU Directive. All animal procedures were performed in accordance with the ARVO Statement for the Use of Animals in Ophthalmic and Vision Research.

Streptozotocin-Induced Diabetic Rat Model

Brown–Norway rats (male, 7 weeks old (Charles River Laboratories, Wilmington, MA, USA) were acclimatized for 3 weeks until their body weight reached 200 to 250 g. All rats were fasted overnight, starting the evening before streptozotocin (STZ) treatment. The rats were briefly anesthetized with isoflurane and were rendered diabetic with one intraperitoneal (IP) injection of STZ (55 mg/kg). Control non-diabetic rats received one IP injection of citric acid monohydrate (CAM) buffer. Body weight and glucose levels (determined by the use of a glucose meter and strips; GlucoMen, A. Menarini Diagnostics, Firenze, Italy) were measured before CAM or STZ injection. Development of diabetes was defined by blood glucose levels higher than 250 mg/dL and was monitored weekly after the STZ injection. Animals with consistently elevated glucose levels throughout the entire experimental phase of the study were considered diabetic.

Sixty rats were included; of these, six rats were injected with CAM and 54 rats were injected with STZ, and all the STZ-injected animals were rendered diabetic within the first week thereafter. Immediately after diabetes onset, treatment was initiated by randomizing the diabetic rats into six treatment groups: (1) single IVT vehicle of THR-149 (n = 10), (2) single IVT THR-149 (n = 10), (3) repeated IVT vehicle of THR-149 (n = 10), (4) repeated IVT THR-149 (n = 10), (5) vehicle of VEGF-Trap (n = 7), and (6) VEGF-Trap (n = 7), which is described as a positive control for evaluating leakage in this model.[23] After sacrifice, the eyes of the animals were further subdivided for collection of retinal sections or retinal whole-mounts.

Compound Administration

Isoflurane was used to induce general anesthesia, and the eye was treated with a drop of tropicamide. Diabetic rats were treated with one (single) or three (repeated) bilateral IVT injections of 12.5 µg per eye of THR-149 or vehicle, with an interval of 1 week between the injections. Of note, the number of three IVT injections was selected to cover the total study duration of 4 weeks. Intravitreal injections (5 µL) were performed by using an analytic science syringe (SGE Analytical Science, Melbourne, Australia) and beveled glass micropipettes (80-µm diameter; Clunbury Scientific, Bloomfield Hills, MI, USA), controlled by the UMP3I Microsyringe Injector and Micro4 Controller (World Precision Instruments, Sarasota, FL, USA). VEGF-Trap (2 mg/kg, positive control) or its vehicle was administered via repeated IP injections (3×/wk) to induce its maximum effect, as previously described,[21,23] starting immediately after diabetes onset until week 3.

Histological Evaluation

At 4 weeks after diabetes onset, microglia/macrophage and Müller cell (re)activation and levels of inflammatory cytokines, Kir4.1 and AQP4 channels, vascular retinal leakage, and retinal thickness were quantified on sections by means of histological evaluation. Both eyes from non-diabetic (n = 10 eyes) and diabetic (n = 14 eyes/group) animals were included, unless stated otherwise.

Collection of Eyes. Intravenous injection (via sublingual vein) of 100 µg/g bovine serum albumin (BSA) conjugated with fluorescein isothiocyanate (FITC; A9771; Sigma-Aldrich, St. Louis, MO, USA) dissolved in PBS (50 mg/mL) was performed in isoflurane-anesthetized rats. Twenty minutes after perfusion, rats were sacrificed by an overdose of pentobarbital (50 mg/mL). Both eyes were enucleated and placed in 1% (v/v) formaldehyde at 4°C overnight (protected from light), after which the eyes were rinsed three times in PBS, stored 2 days in 70% (v/v) ethanol, dehydrated, and then embedded in paraffin wax. Retinal sections (9 µm) were collected in series of five glass slides. The first slide was stained with hematoxylin and eosin (H&E) for assessment of the retinal morphology, whereas consecutive slides were used for different immunostainings.

Immunohistochemistry. Immunohistochemical investigation of different markers was performed in all eyes (n = 10–14 per group for ionized calcium binding adaptor molecule [Iba1] and vimentin) or in a subset of eyes (n = 4–11 for IL-1β, IL-6, Kir4.1, and AQP4). Sections were incubated overnight with primary antibody for Iba1 (1/800; 019-19741; Sopachem, Ede, Netherlands), vimentin (1/400; V5255; Sigma-Aldrich), IL-6 (1/250; ab9324; Abcam, Cambridge, UK), IL-1β (1/1000; ab9722; Abcam), Kir 4.1 (1/200; APC-035; Alomone Labs, Jerusalem, Israel), or AQP4 (1/200; AQP-004; Alomone Labs). The following day, the secondary antibodies were added for 45 minutes: Peroxidase AffiniPure Goat Anti-Rabbit IgG (H+L) for Iba1 and

IL-1β (1/100; 111-035-144; The Jackson Laboratory, Bar Harbor, ME); for vimentin and IL-6, Biotin-SP (long spacer) AffiniPure Donkey Anti-Mouse IgG (H+L) (1/300; 715-065-151; The Jackson Laboratory); or, for Kir4.1 and AQP4, Invitrogen Goat Anti-Rabbit IgG (H+L) Highly Cross-Adsorbed Secondary Antibody, Alexa Fluor 568 (1/200; A-11036; Thermo Fisher Scientific, Waltham, MA, USA). The antibody complexes were visualized using an amplifier kit (1/50; TSA Cyanine 3 Kit; PerkinElmer, Waltham, MA, USA), and slides were mounted with ProLong Gold Antifade Mutant with DAPI (4′,6-diamidino-2-phenylindole; P36935; Thermo Fisher Scientific).

Vascular Leakage and Retinal Thickness. FITC-BSA–perfused slides of all eyes (n = 10–14 per group) were dewaxed and mounted with ProLong Gold with DAPI to measure fluorescent intensity for the assessment of retinal vessel leakage. These slides were also used for measuring the entire retinal thickness, from the internal limiting membrane (ILM) to the photoreceptor layer (PRL), and the thickness of the following individual retinal layers: ganglion cell layer (GCL) complex, including the ILM, retinal nerve fiber layer, and GCL; inner plexiform layer (IPL); inner nuclear layer (INL); outer plexiform layer (OPL); outer nuclear layer (ONL); and PRL (i.e., inner and outer segments of the PR cells).

Quantitative Fluorescent Microscopic Analysis

Microscopic analysis was performed by a masked observer on six cross-sections in total: three sections under and three sections above the optic nerve. Cross-sections that included the optic nerve head were excluded. Fluorescent images of each of the six retinal sections in the central retina, including all retinal layers, were collected (two images at each section). All immunohistochemical analyses were performed 50 µm from the optic nerve head, and in total the measurements obtained from 12 images were averaged and assessed with a fluorescence microscope and ZEN software (Zeiss, Oberkochen, Germany).

Areas in the retina positive for Iba1, IL-6, IL-1β, vimentin, and Kir4.1 were investigated by measuring the ratio of the immunopositive area over the retinal area per image, whereas the AQP4-positive area was measured over the ONL area and expressed as a percentage. Iba1-positive cells were counted in two standard areas (~500 µm of length) per image, including all retinal layers, and were further classified based on their morphology, as previously described.[24–26] Ramified non-activated immune cells were defined as having a small, round soma and various branched thin processes, whereas amoeboid activated cells had enlarged soma with shortening and widening of the processes.

Vascular leakage was assessed by measuring the retinal fluorescent intensity (with exclusion of the retinal blood vessels) by placing different rectangles on the entire retina in between the blood vessels, as previously described.[27] The fluorescent intensity values of each rectangle were averaged in order to obtain one value per image. The retinal fluorescent intensity per image was further normalized to the background fluorescent intensity on the slide for measuring the leakage (by calculating the difference between retina and background values). The retinal thickness was measured at three different locations covering the entire retina or the individual retinal layers (i.e., GCL, IPL, INL, OPL, ONL, and PRL). The measurements were further averaged to obtain one value per image.

Retinal Whole-Mount Staining

At 4 weeks after diabetes onset, retinal whole-mounts were collected from non-diabetic (n = 2 eyes) and diabetic rats treated with vehicle or THR-149 (n = 3 eyes per group). Rats were sacrificed, and the eyes were enucleated and placed in 1% (v/v) formaldehyde at 4°C overnight (protected from light), after which the eyes were rinsed in PBS. Retinas were dissected and stored in PBS after a post-fixation step for 1 hour at room temperature in 4% formaldehyde. Flat-mounts were incubated overnight with rabbit-anti-mouse Iba-1 (1/1000; 019-19741; FUJIFILM Wako Chemicals Europe, Neuss, Germany) or mouse anti-rat CD68 (1/500; MCA341GA; Bio-Rad AbD Serotec Ltd., Oxford, UK), followed by incubation in the dark for 2 hours at room temperature with Invitrogen Goat Anti-Rabbit IgG (H+L) Highly Cross-Adsorbed Secondary Antibody, Alexa Fluor 488 (1/200; A-11034; Thermo Fisher Scientific) or Invitrogen Goat Anti-Mouse IgG (H+L) Highly Cross-Adsorbed Secondary Antibody, Alexa Fluor 594 (1/500; A11032; Thermo Fisher Scientific), respectively. Flat-mounts were mounted with VECTASHIELD Vibrance Antifade Mounting Media without DAPI (H-1700; Vector Laboratories, Burlingame, CA, USA). Mosaic Z-stack images of the Iba1 staining, from the nerve fiber layer until the ONL (step size, 4 µm), of two quarters of each retina were taken with a multiphoton microscope (FV1000; Olympus, Tokyo, Japan) with a 20× objective. Next, various morphological parameters—mean nearest neighbor distance (NND), the space between cells; regularity index, the regularity of cell spacing; and soma size and roundness—were analyzed as described in Davis et al.[28] Three images of CD68/Iba-1 co-staining were taken in the center and periphery of one quarter of each retina with a 63× objective and a confocal microscope (SP5; Leica, Wetzlar, Germany).

Statistical Analysis

All graphing and statistical analysis was performed using Prism 6 (GraphPad Software, San Diego, CA, USA) to determine statistical significance (*P < 0.05; **P < 0.01; ***P < 0.001). Statistical analysis comparing the effects of all of the groups was performed with a one-way ANOVA using a Bonferroni post hoc test. Data from one experiment are presented in the graphs as mean ± SEM and were confirmed in a second, identical, independent replicate experiment (including similar treatment groups and number of animals), for which the data are not shown.

Results

Weight and Blood Glucose Levels

Weight and blood glucose levels were determined before and after STZ injection (week 0). Body weight increased in all CAM-treated rats from week 1 until week 4 and was significantly higher as compared with the rats that were treated with STZ (P < 0.01). This difference in weight can be explained by the diabetic phenotype. Indeed, analysis of blood glucose measurements showed that the STZ-treated rats showed significantly increased glucose levels (>250 mg/dL) from week 1 onward as compared with CAM-treated rats (P < 0.001). The diabetes-induced weight loss or increased glucose levels were not significantly changed after treatment with VEGF-Trap or THR-149 (P > 0.05 compared

Investigative Ophthalmology & Visual Science

Table 1. Average Body Weight and Glucose Measurements in Non-Diabetic and Diabetic Rats (Mean ± SEM)

	Body Weight (g)					Blood Glucose Level (mg/dL)				
Weeks After STZ	**0**	**1**	**2**	**3**	**4**	**0**	**1**	**2**	**3**	**4**
Non-diabetic ($n = 6$)	258 ± 6	269 ± 7	278 ± 8	290 ± 9	298 ± 8	126 ± 3	103 ± 10	117 ± 1	116 ± 1	120 ± 3
Diabetic ($n = 54$)										
Vehicle VEGF-Trap ($n = 7$)	258 ± 4	239 ± 4	251 ± 4	246 ± 5	244 ± 4	118 ± 2	459 ± 10	482 ± 13	508 ± 5	520 ± 21
VEGF-Trap ($n = 7$)	263 ± 7	243 ± 4	250 ± 5	248 ± 4	241 ± 3	120 ± 1	437 ± 25	519 ± 19	557 ± 15	539 ± 17
Vehicle THR-149; single ($n = 10$)	249 ± 5	228 ± 5	237 ± 6	238 ± 7	240 ± 9	118 ± 1	452 ± 17	477 ± 12	500 ± 14	510 ± 8
THR-149; single ($n = 10$)	258 ± 5	237 ± 5	243 ± 7	245 ± 7	244 ± 7	120 ± 2	445 ± 15	462 ± 16	501 ± 17	491 ± 13
Vehicle THR-149; repeated ($n = 10$)	254 ± 4	238 ± 4	245 ± 4	242 ± 5	244 ± 5	120 ± 1	472 ± 19	485 ± 16	491 ± 19	499 ± 18
THR-149; repeated ($n = 10$)	258 ± 4	236 ± 6	243 ± 6	242 ± 8	239 ± 7	117 ± 3	461 ± 8	482 ± 16	488 ± 15	483 ± 21

with vehicle-treated diabetic rats). Average body weight and blood glucose values are presented in Table 1.

Retinal Inflammation

Microglia/Macrophage Activation. Analysis of the Iba1 staining on retinal sections following 4 weeks of diabetes showed a significant increase in the Iba1-positive area when compared with non-diabetic controls ($P < 0.01$). This increase was significantly reduced back to baseline by administration of VEGF-Trap ($P < 0.01$ vs. vehicle VEGF-Trap). A single injection of 12.5 µg/eye of THR-149 induced a reduction in the positive area of 61% ± 8% ($P < 0.001$ vs. 1× IVT vehicle). Repeated injections of THR-149 produced a 51% ± 11% decrease ($P < 0.05$ compared with 3× administration of the vehicle) (Figs. 1A–1D). The total number of Iba1-positive cells and the number of activated immune cells were also significantly increased in the diabetic retina, as compared with control eyes ($P < 0.05$ and $P < 0.01$, respectively). This diabetes-induced increase in cell count was significantly reduced to baseline levels after VEGF-Trap, single or repeated administration of THR-149 ($P < 0.05$ as compared with vehicle-treated eyes) (Figs. 1B, 1C). Analysis of the Iba1-stained retinal whole-mounts showed a significantly decreased NND in the diabetic eyes as compared with non-diabetic control eyes ($P < 0.05$). The spacing between the immune cells became larger again after repeated administration of THR-149 versus vehicle ($P < 0.05$) (Fig. 2). Iba1-stained retinal whole-mounts were further stained for CD68 for morphological assessment of the activated immune cells. CD68 is known to be expressed in high levels by macrophages and activated microglia and in low levels by resting microglia.[29] Qualitative evaluation did show more $CD68^+/Iba1^+$ amoeboid microglia in the diabetic eyes treated with vehicle of THR-149 as compared with non-diabetic control eyes. Administration of both single and repeated THR-149 did result in more $CD68^-/Iba1^+$

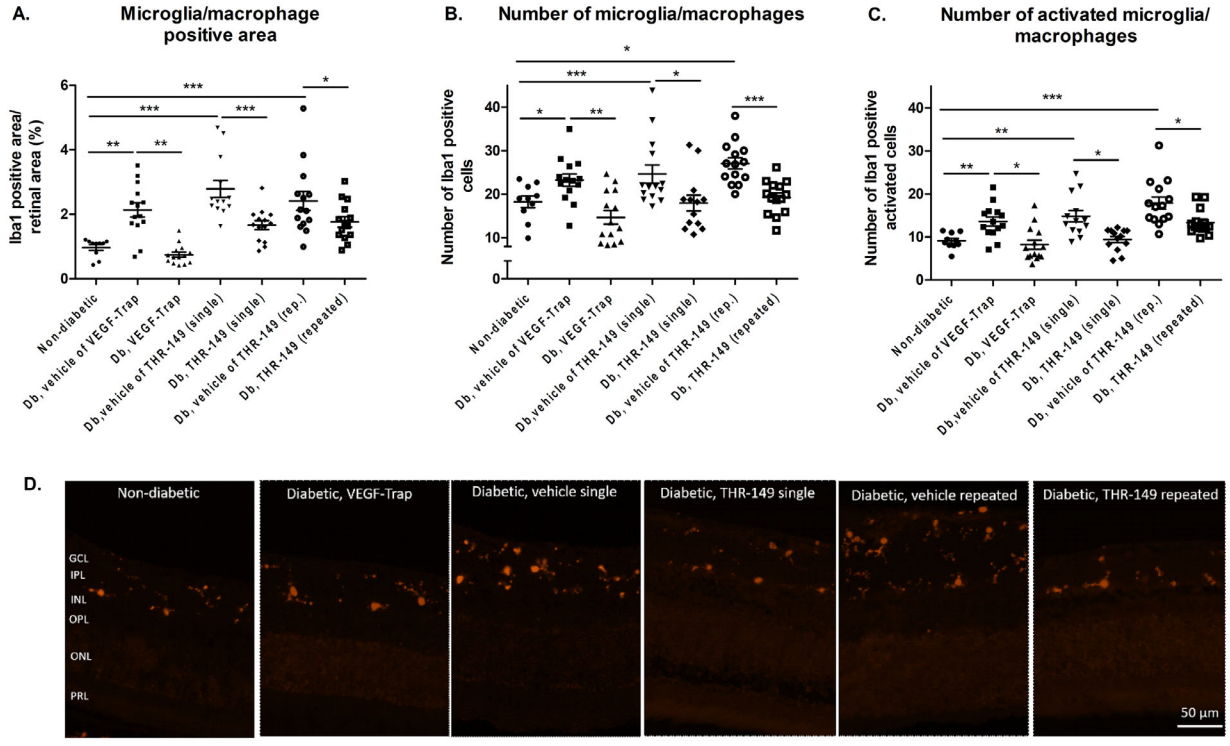

Figure 1. The activation of retinal microglia and macrophages was decreased after single and repeated THR-149 administration. (**A–C**) Representative graphs and (**D**) images demonstrating a significant decrease in the Iba1-positive retinal area, total number of Iba1-positive cells, and number of activated cells, after single and repeated administration of THR-149 at 4 weeks after diabetes onset versus vehicle ($n = 10$ eyes for non-diabetic and $n = 13$ or 14 eyes for diabetic groups). Individual data points and mean ± SEM are shown. *$P < 0.05$; **$P < 0.01$; ***$P < 0.001$. *Scale bar*: 50 µm. Db, diabetic; rep, repeated.

Investigative Ophthalmology & Visual Science

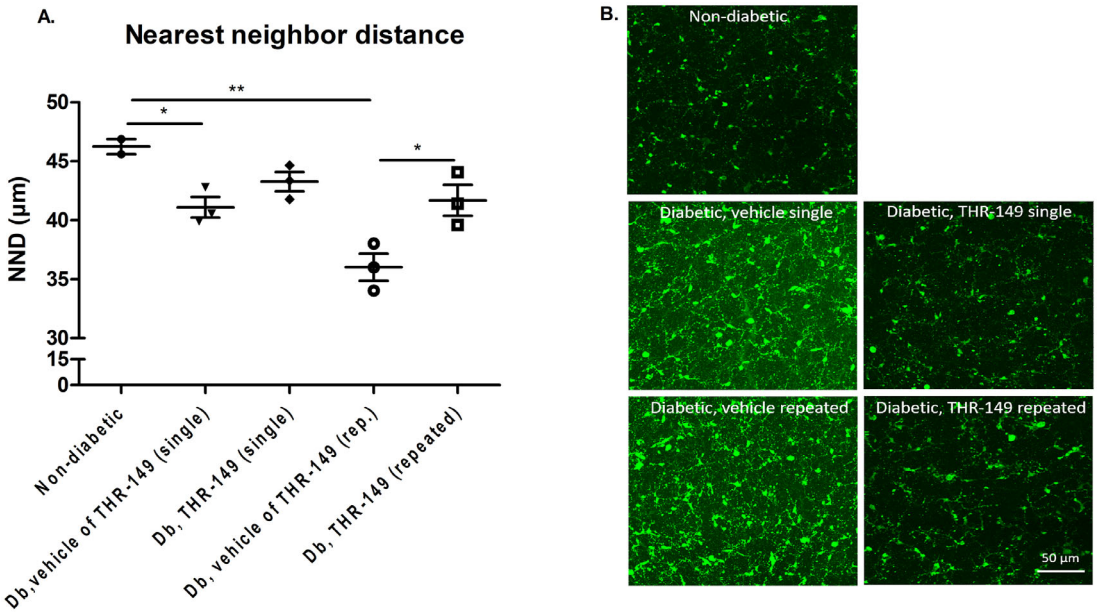

Figure 2. The NND increased after single and repeated THR-149 administration. (**A**) The NND measured in Iba1-stained retinal whole-mounts was significantly increased after THR-149 administration at 4 weeks after diabetes onset as compared with vehicle ($n = 2$ eyes for non-diabetic and $n = 3$ eyes for all diabetic groups). Individual data points and mean ± SEM are shown. *$P < 0.05$; **$P < 0.01$. (**B**) Representative images of Iba1-stained retinal whole-mounts after THR-149 treatment. *Scale bar*: 50 µm.

ramified cells as compared with vehicle, indicating the reduction of activated immune cells in the diabetic retina after administration of the PKal inhibitor (Fig. 3).

Inflammatory Cytokines. To further unravel how THR-149 could potentially exert its anti-inflammatory effect, the levels of proinflammatory cytokines IL-6 and IL-1β in the diabetic retina were investigated by means of histological evaluation on retinal sections. The levels of both cytokines were increased after diabetes (vs. control animals), and administration of single and repeated THR-149 significantly decreased the diabetes-induced retinal levels of IL-6 by 78% ± 9% and 55% ± 13%, respectively ($P < 0.05$ vs. vehicle). This effect was similar to the effect induced after VEGF-Trap administration ($P < 0.01$ vs. vehicle) (Fig. 4).

Reactive Gliosis

Reactive gliosis (i.e., activation of macroglial cells) was investigated by measuring the area of retina covered by vimentin-positive Müller cells and astrocytes, which were significantly increased in diabetic animals compared with non-diabetic controls ($P < 0.05$). Treatment of diabetic rats with VEGF-Trap led to a reduction back to baseline in gliosis ($P < 0.05$ vs. VEGF-Trap vehicle). Repeated administration of THR-149 also reduced the appearance of vimentin-positive cells in diabetic rats back to levels comparable to those of non-diabetic controls ($P < 0.05$ compared to 3× vehicle). In contrast, there was no significant difference following a single administration of 12.5 µg/eye of THR-149 ($P = 0.99$ vs. single vehicle) (Fig. 5).

Potassium- and Water Homeostasis–Related Channels

Inwardly Rectifying Potassium Channel Subunit Kir4.1. The expression of the major potassium channel of the Müller cells was studied by analyzing the Kir4.1-positive retina area. At 4 weeks following the induction/onset of diabetes, the retina showed a decrease in the Kir4.1-positive area as compared with non-diabetic eyes ($P < 0.001$), which was partially but significantly improved by VEGF-Trap by 46% ± 16% ($P < 0.05$ vs. VEGF-Trap vehicle). A single THR-149 administration had no significant effect on the Kir4.1-positive area ($P = 0.65$ vs. vehicle), whereas repeated IVT of THR-149 restored Kir4.1 protein levels in the diabetic retina back to baseline ($P < 0.01$ vs. vehicle and $P < 0.05$ vs. single THR-149) (Fig. 6).

AQP4-Positive Water Channels. The expression of water channels of the Müller cells was studied by analyzing the AQP4-positive area. Diabetic eyes showed an increase in the AQP4-positive ONL area as compared with the non-diabetic eyes ($P < 0.05$), but none of the test compounds significantly reduced the AQP4-positive area ($P > 0.05$ vs. their vehicles) (Fig. 7) over the experimental time frame.

Vascular Leakage

Retinal vascular permeability was significantly increased after STZ induction ($P < 0.05$ as compared with non-diabetic rats) and was significantly reduced by 73% ± 23% after VEGF-Trap and 65% ± 12% after repeated THR-149 administration ($P < 0.05$ vs. their vehicle). The vascular leakage observed after a single administration of 12.5 µg/eye of THR-149 was not significantly different from its vehicle ($P = 0.94$) (Fig. 8), although both groups were associated with a higher level of variability.

Retinal Thickness

Total Retinal Thickness. Total retinal thickness was investigated at week 4 after diabetes onset on histological sections. Diabetic rats showed a significant increase in retinal thickness as compared with non-diabetic rats, without any apparent loss of neuronal cells. A reduction of

Investigative Ophthalmology & Visual Science

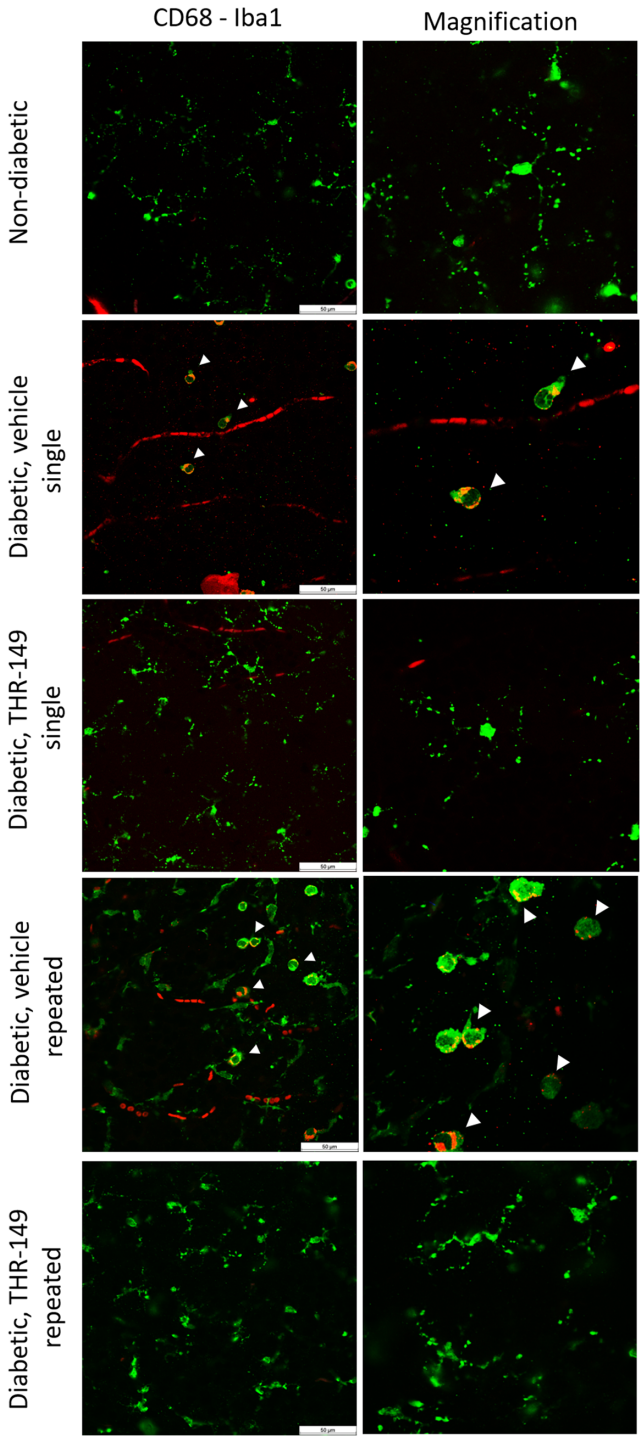

Figure 3. Representative CD68- and Iba1-stained retinal whole-mounts of the different treatment groups at 4 weeks after diabetes onset. Representative images of CD68-stained (*red*) and Iba1-stained (*green*) retinal whole-mounts indicating more $CD68^{+}/Iba1^{+}$ amoeboid microglia in the diabetic eyes treated with vehicle of THR-149 (indicated with the *white arrowhead*) as compared with non-diabetic control eyes. Administration of THR-149 did result in more $CD68^{-}/Iba1^{+}$ ramified cells as compared with vehicle eyes. The images on the *right* are higher magnification. *Scale bar*: 50 µm.

42 ± 4.9 µm in retinal thickness was observed after repeated administration of VEGF-Trap ($P < 0.001$ vs. vehicle of VEGF-Trap). A single administration of 12.5 µg/eye of THR-149 did not induce a significant decrease in retinal thickness ($P = 0.30$ vs. vehicle), whereas repeated IVT injections of the PKal-inhibitor reduced thickening of the total retina by 50 ± 12 µm versus vehicle ($P < 0.05$). The effect of repeated injections of THR-149 was also significantly different compared with single administration of this PKal inhibitor ($P < 0.05$) (Figs. 9, 10).

Retinal Layer Thickness. Analysis of individual retinal layers revealed that diabetes did not affect the thickness of the GCL and OPL, but changes were induced for the IPL, INL, ONL, and PRL. These layers showed significant increases of 15 ± 2.4 µm, 6.3 ± 0.3 µm, 27 ± 1.0 µm, and 9.3 ± 1.3 µm, respectively, 4 weeks after diabetes onset ($P < 0.05$ vs. non-diabetic rats). A single IVT injection of THR-149 did not significantly reduce the thickness of any of these layers ($P > 0.05$ vs. vehicle), although a trend toward reduction of the ONL was observed ($P = 0.06$). Repeated administration of THR-149 and VEGF-Trap, on the other hand, significantly reduced the thickness of the IPL, INL, ONL, and PRL to baseline levels ($P < 0.01$, compared with vehicle-treated rats). Compared to a single IVT administration of THR-149, multiple IVT injections showed a significant difference in all of the retinal layers from which thickness was increased after diabetes ($P < 0.05$) (Table 2).

Discussion

The current standard of care in clinical practice for DME is anti-VEGF therapy, and for most patients there is a significant improvement in visual acuity and reduced retinal thickness. However, treatment response can be variable,[5,6] and other factors beyond VEGF may be involved in patient-linked responses and in disease progression.[30] There is also conflicting evidence on the effect of VEGF inhibitors on inflammatory processes in the edematous retina, as levels of intraocular proinflammatory cytokines after treatment are variable.[31,32] Therefore, there is a clear need for alternative therapies for DME, especially for the suboptimal responders to anti-VEGF therapy.[4]

The goal of this study was to investigate the therapeutic potential and mechanism of THR-149, a recently described bicyclic peptide PKal inhibitor,[21] on several hallmarks of DR, especially those relating to edema. The in vivo efficacy of the inhibitor was tested in the STZ-induced diabetic rat model, one of the most common induced DR models that has been routinely used in fundamental studies and therapeutic drug experiments.[33,34] The model is characterized by increased vitreous/retinal levels of PKal and other components of the KKS,[10,11] and administration of PKal or BK agonists has been shown to further increase diabetes-induced retinal thickening.[12,15] The time point of 4 weeks after diabetes onset to investigate retinal changes was selected based on the peak of diabetes-induced vascular leakage, as well as on reports of increased retinal thickness from 3.5 weeks after diabetes induction.[35,36] Retinal thinning and neurodegeneration leading to depletion of defined neurons across the retinal layers, on the other hand, have been found to peak between 13 and 30 weeks after diabetes onset.[37–39] Although the retinal thickness increase in diabetic rats (on average, 10–20 µm or 10%[35,36]) is not as pronounced compared with diabetic patients (on average 100 µm or 40%[40]), and rats do not have a distinct macular region,[41] retinal thickness measurements in

Investigative Ophthalmology & Visual Science

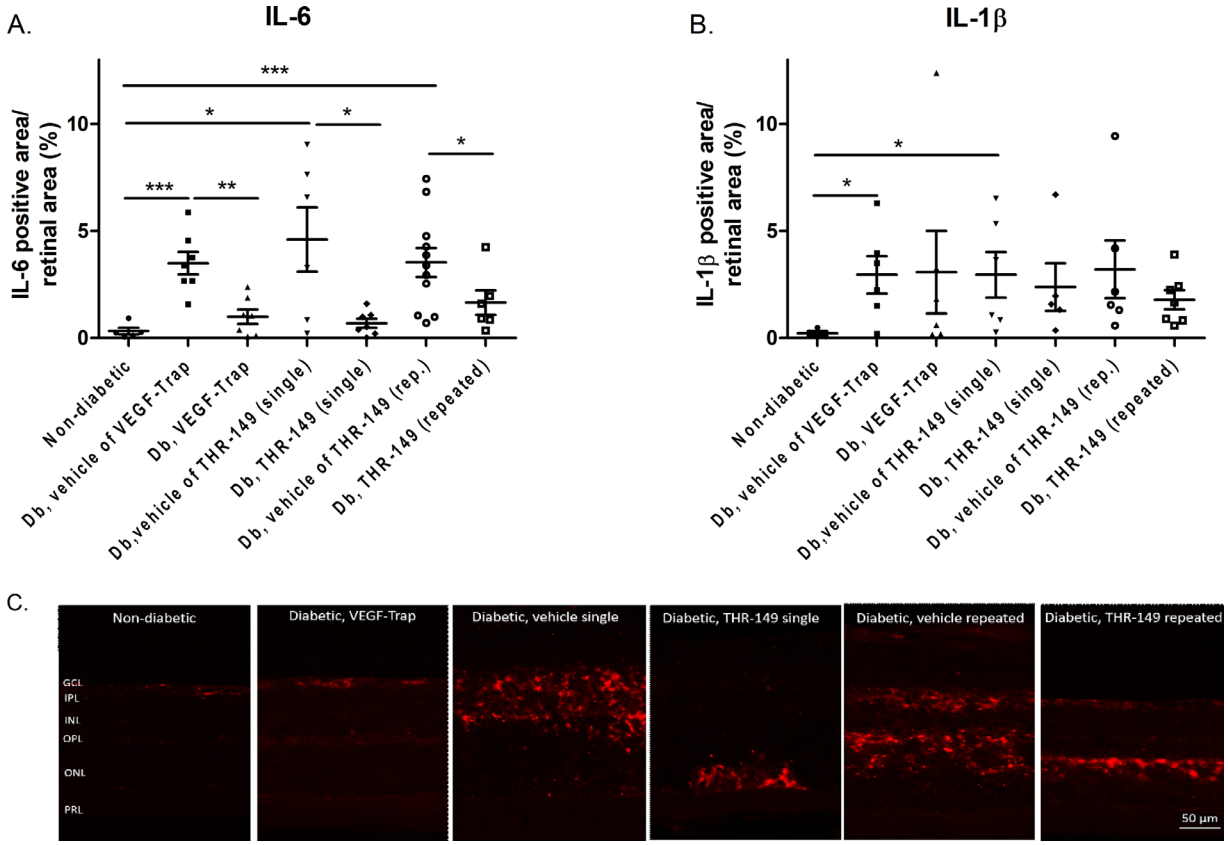

Figure 4. The retinal level of IL-6 decreased after single and repeated THR-149 administration. (**A**) Representative graphs demonstrating that the retinal levels of IL-6 and IL-1β were increased after diabetes and that single and repeated injections of THR-149 significantly decreased the diabetes-induced retinal levels of IL-6 at 4 weeks after diabetes onset as compared with vehicle ($n = 4$ or 5 eyes for non-diabetic and $n = 7$–11 eyes for diabetic groups). Individual data points and mean ± SEM are shown. *$P < 0.05$; **$P < 0.01$; ***$P < 0.001$. (**B**) Representative images of IL-6–stained retinal sections after THR-149 treatment. *Scale bar*: 50 µm.

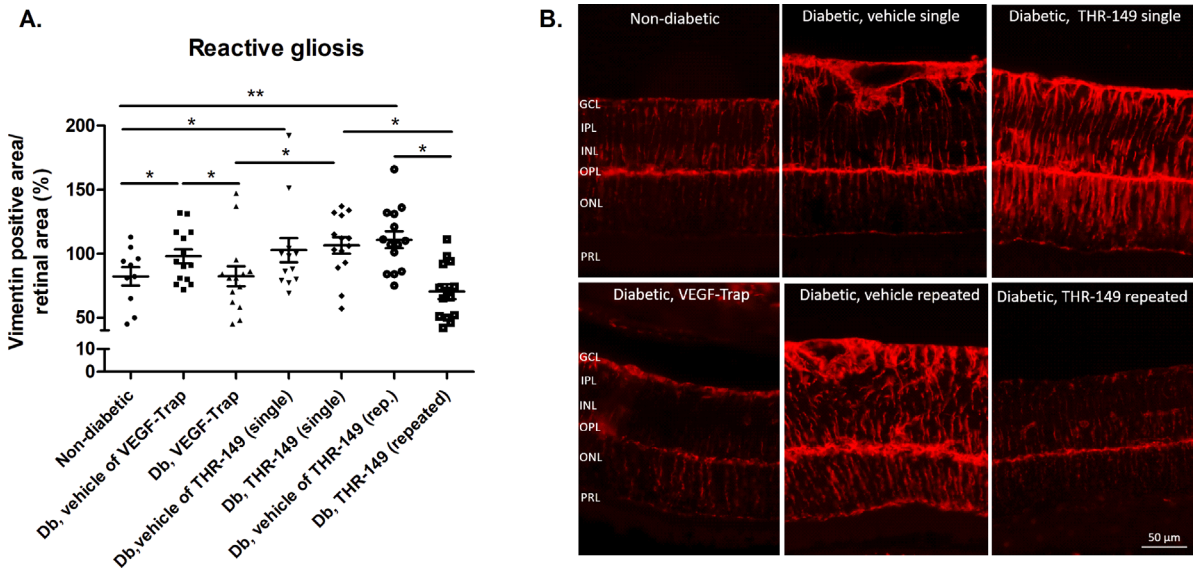

Figure 5. The activation of macroglia was reduced after repeated THR-149 administration, but not after a single IVT injection of the PKal inhibitor. (**A**) Representative graph and (**B**) images demonstrating a significant decrease in the vimentin positive retinal area after repeated administration of THR-149 at 4 weeks after diabetes onset. A single IVT injection of the PKal inhibitor did not induce a significant reduction in reactive gliosis compared with its vehicle ($n = 10$ eyes for non-diabetic and $n = 13$ or 14 eyes for diabetic groups). Individual data points and mean ± SEM are shown. *$P < 0.05$; **$P < 0.01$. *Scale bar*: 50 µm.

Investigative Ophthalmology & Visual Science

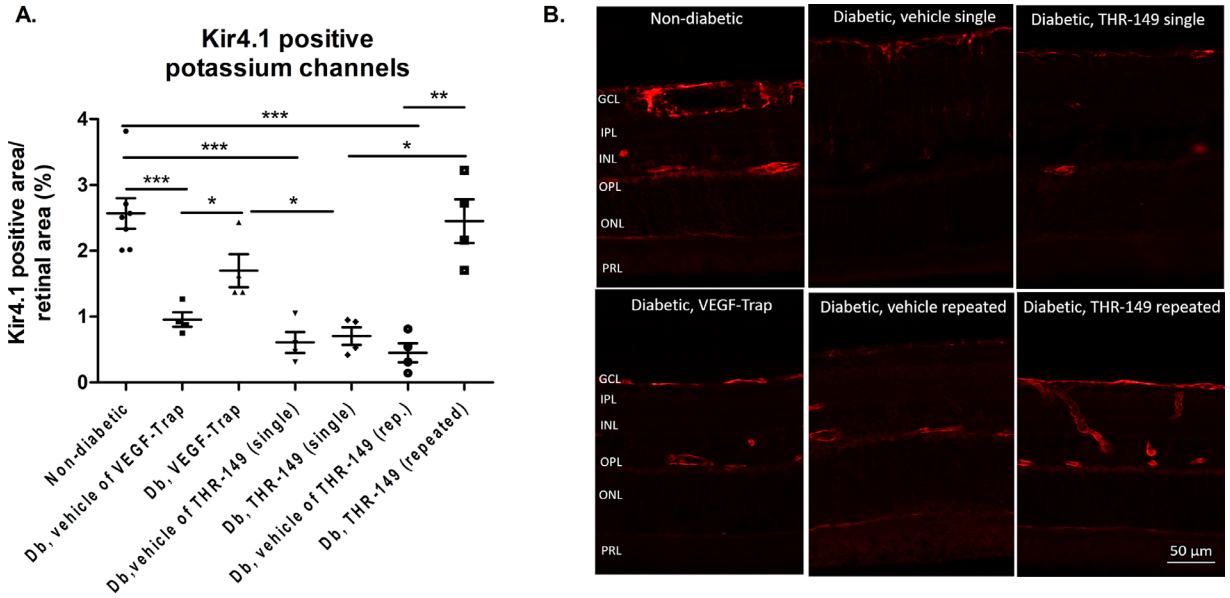

Figure 6. The diabetes-induced decrease in Kir4.1-positive potassium channels level was restored after repeated THR-149 administration. (**A**) Representative graph and (**B**) images demonstrating a significant increase in the Kir4.1-positive retinal area after repeated administration of THR-149 at 4 weeks after diabetes onset. A single IVT injection of the PKal inhibitor did not significantly change the Kir4.1-positive retinal area compared with its vehicle ($n = 7$ eyes for non-diabetic and $n = 4$ eyes for all diabetic groups). Individual data points and mean ± SEM are shown. *$P < 0.05$; **$P < 0.01$; ***$P < 0.001$. *Scale bar*: 50 µm.

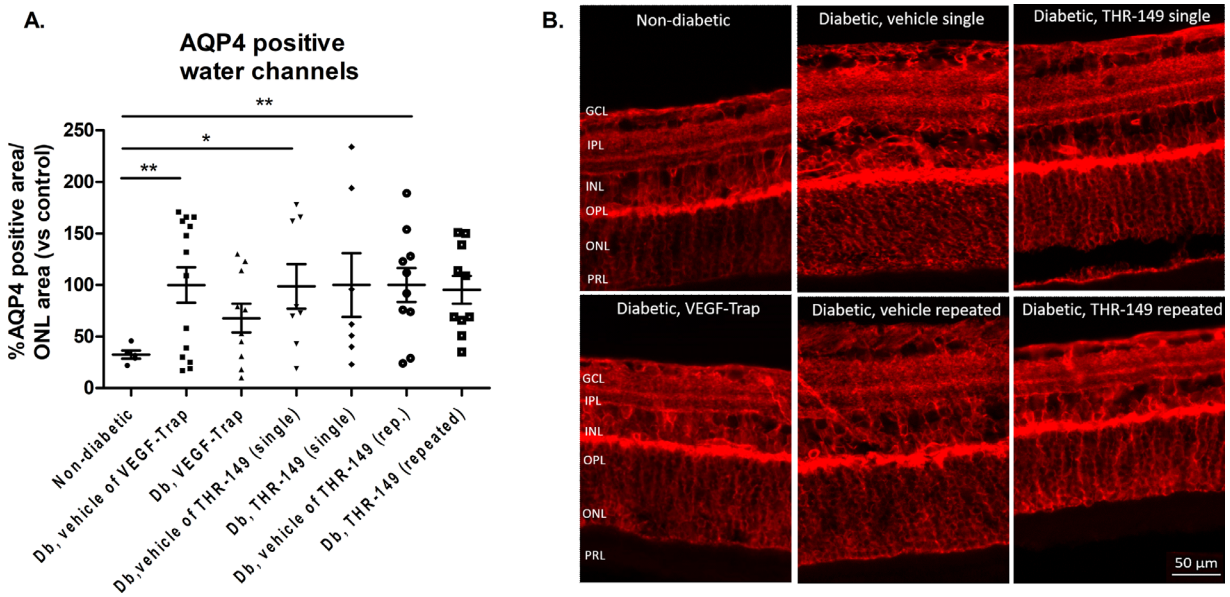

Figure 7. Repeated THR-149 administration did not reduce the increased levels of AQP4-positive water channels in the diabetic retina. (**A**) Representative graph and (**B**) images demonstrating no change in the AQP4-positive ONL area after single and repeated administration of THR-149 at 4 weeks after diabetes onset ($n = 5$ eyes for non-diabetic and $n = 7$–14 eyes for diabetic groups). Individual data points and mean ± SEM are shown. *$P < 0.05$; **$P < 0.01$. *Scale bar*: 50 µm.

the diabetic rat are still relevant as a preclinical read-out with relevance to the clinical situation. Indeed, optical coherence tomography analysis of the central/foveal retinal thickness is considered a clinical standard procedure to diagnose DME.[40] In addition, it is also considered to be of key importance to determine the effectiveness of pharmacological treatment of the disease.

In this study, repeated IVT injections of THR-149 significantly reduced diabetes-induced retinal thickening and vascular leakage, confirming the earlier described anti-leakage effects of THR-149 (Van Bergen T et al.[68]). Specifically, repeated injections reduced the thickness of the IPL, INL, ONL, and PRL, which is in line with what has been described in the literature using prekallikrein-deficient

Investigative Ophthalmology & Visual Science

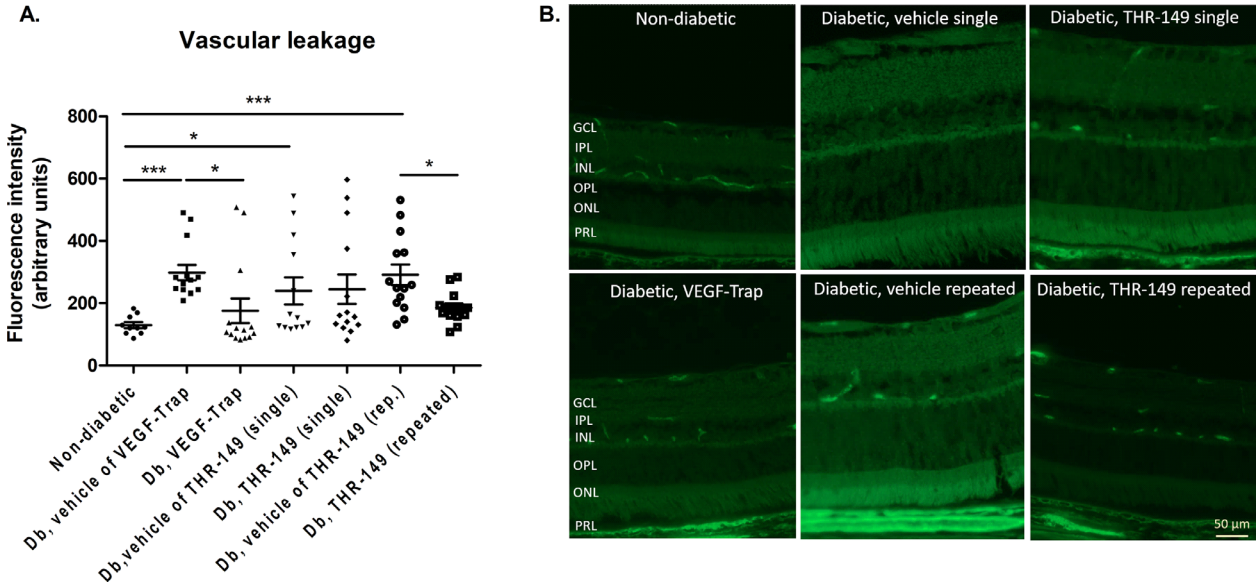

Figure 8. Repeated IVT injections of THR-149 reduced retinal vascular leakage, whereas single administration did not. (**A**) Representative graph and (**B**) images demonstrating significant reduction of retinal vascular leakage after repeated administration of THR-149 at 4 weeks after diabetes onset ($P < 0.05$ vs. vehicle), whereas a single IVT injection of the PKal inhibitor did not induce any changes compared with its vehicle ($n = 10$ eyes for non-diabetic and $n = 13$ or 14 eyes for diabetic groups). Individual data points and mean ± SEM are shown. *$P < 0.05$; ***$P < 0.001$. *Scale bar*: 50 µm.

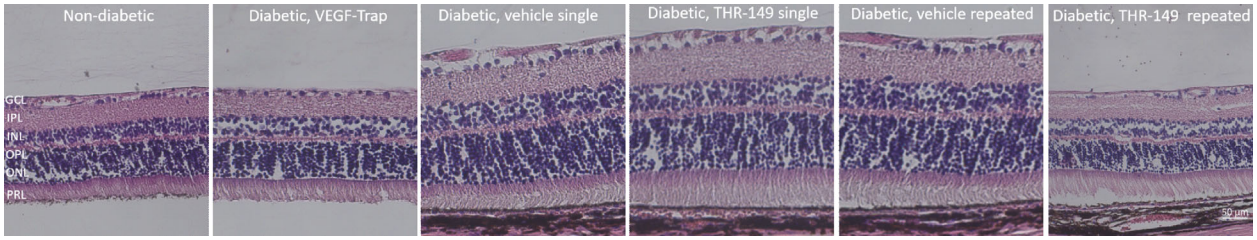

Figure 9. Representative H&E images of the different treatment groups at 4 weeks after diabetes onset.

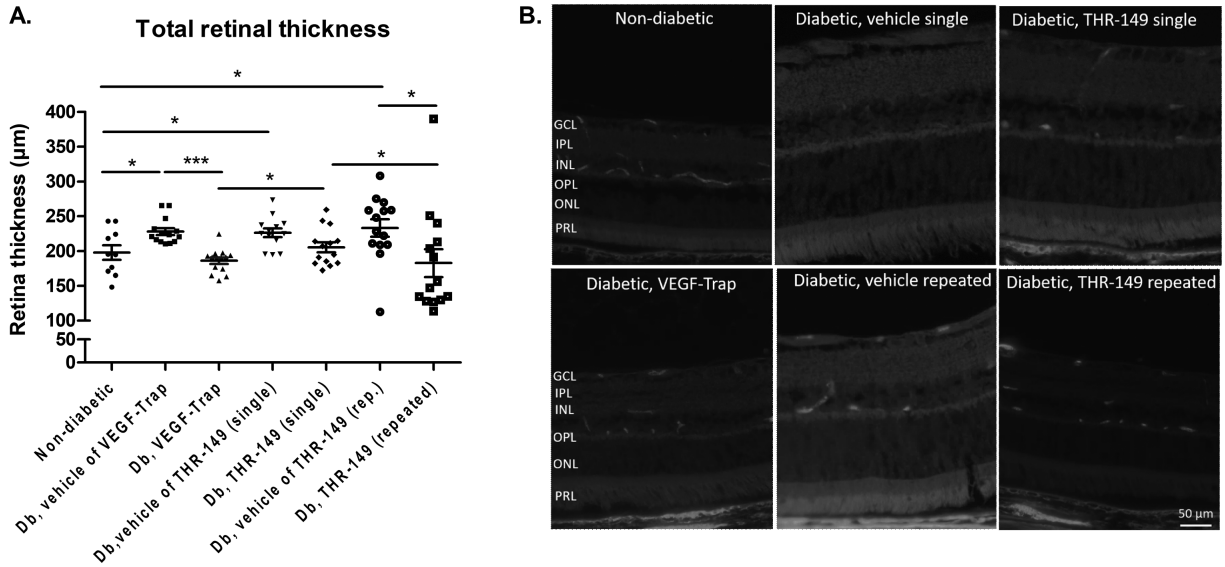

Figure 10. Repeated administration of THR-149 significantly reduced total retinal thickening, whereas single administration did not. (**A**) Representative graph and (**B**) images demonstrating significant reduction of retinal thickening after repeated IVT administration of THR-149 at 4 weeks after diabetes onset. Single IVT administration of the PKal inhibitor did not significantly reduce retinal thickness ($P = 0.30$ vs. vehicle) and was significantly different as compared with repeated THR-149 ($n = 10$ eyes for non-diabetic and $n = 13$ or 14 eyes for diabetic groups). Individual data points and mean ± SEM are shown; *$P < 0.05$; ***$P < 0.001$. *Scale bar*: 50 µm.

Investigative Ophthalmology & Visual Science

Table 2. Average Thickness (µm) of the Individual Retinal Layers (Mean ± SEM)

	Treatment Group						
Layer	Non-Diabetic	Diabetic, Vehicle VEGF-Trap	Diabetic, VEGF-Trap	Diabetic, Vehicle THR-149 (Single)	Diabetic, THR-149 (Single)	Diabetic, Vehicle THR-149 (Repeated)	Diabetic, THR-149 (Repeated)
GCL	13 ± 1.1	14 ± 0.7	12 ± 0.9	16 ± 1.0	15 ± 0.7	14 ± 1.4	12 ± 0.6
IPL	38 ± 2.5	49 ± 2.0*	37 ± 2.6†	51 ± 4.9*	49 ± 3.0	57 ± 5.1*	32 ± 2.5‡,§
INL	21 ± 2.2	27 ± 1.3*	20 ± 1.9†	28 ± 2.0*	25 ± 1.8	28 ± 2.0*	19 ± 1.9‡,§
OPL	8.5 ± 0.5	10 ± 0.5	8.2 ± 0.7	8.8 ± 0.7	8.4 ± 0.6	12 ± 1.5	7.2 ± 0.7
ONL	40 ± 1.8	66 ± 1.7*	44 ± 1.6†,§	69 ± 3.6*	59 ± 3.1*	66 ± 4.3*	40 ± 1.1‡,§
PRL	30 ± 2.3	38 ± 1.8*	25 ± 2.2†,§	38 ± 2.3*	38 ± 3.4	42 ± 3.2*	24 ± 1.9‡,§

* $P < 0.05$ versus non-diabetic.
† $P < 0.05$ versus vehicle of VEGF-Trap.
‡ $P < 0.01$ versus vehicle THR-149 (repeated).
§ $P < 0.05$ versus single THR-149.

(KLKB1$^{-/-}$) mice and after the use of a PKal inhibitor in a VEGF-induced model of retinal vascular leakage.[17] Although differently administrated, the effect of repeated IVT injections of THR-149 could induce effects similar to those of systemic administration of VEGF-Trap (3×/wk to induce its maximum effect[21,23]). On the other hand, single administration of THR-149 was not able to significantly decrease vascular leakage, nor thickness of the total retina or specific retinal layers, as compared with its vehicle. It is unlikely that the lack of significant efficacy of a single IVT injection can be explained by insufficient target engagement due to the fast clearance after local ocular administration in the small rat eye,[42,43] because a single injection of THR-149 in week 1 produced a significant reduction in the inflammation response at 4 weeks after diabetes onset. These findings highlight the need for repeated IVT injections of THR-149 in order to affect diabetes-induced retinal thickening.

How inhibition of PKal leads to this reduced retinal leakage and thickening has not been studied in detail. Therefore, first the anti-inflammatory effect of THR-149 was investigated, showing that both single and repeated IVT injections of THR-149 significantly decreased the retinal inflammatory area, as well as the number of total and activated microglia and/or blood-borne macrophages. Activation of innate immune cells is a key aspect of the inflammatory response in the diabetic retina[44] and has been reported to be linked to macular edema in patients.[45,46] It is one of the first processes that is induced after STZ injection (i.e., week 1–2 post-diabetes), preceding increased vessel leakage and retinal thickening (i.e., week 4 post-diabetes), which can explain the anti-inflammatory effect of a single IVT injection in week 1. In addition to activation of the innate immune cells, an increase in proinflammatory cytokines has also been described in the eyes of DME patients[47–49] and is known to be an important early pro-inflammatory response in diabetes.[50–52] Moreover, the release of cytokines (e.g., IL-6, IL-1β) is described to be involved in the induction of B1R via activation of the nuclear factor kappa B (NF-κB) pathway.[53–56] The use of B1R antagonists did show reduced IL-1β levels in preclinical (diabetic) animal models,[20,57] and IL-6 has been described to be upregulated after bradykinin administration in an in vitro assay,[58] all indicating a potential link between these cytokines and the kallikrein–kinin pathway. Administration of THR-149 decreased the diabetes-induced retinal levels of IL-6, which can potentially explain the reduced activation state of the myeloid cells observed after administration of the PKal inhibitor. Although retinal anti-inflammatory effects have already been described in the literature for B2R[59] or B1R[20] antagonists, this is the first study, to our knowledge, that demonstrates retinal anti-inflammatory effects for a pure PKal inhibitor.

Next, diabetes-induced retinal thickening has also been reported to be linked to Müller cell swelling, leading to decreased clearance/drainage of fluid.[60] Müller cells are indeed involved in retinal water homeostasis, which is mainly regulated by the inwardly rectifying potassium Kir4.1 channel and AQP4 water channel, both expressed on Müller cells.[61] Upon retinal stress, such as in diabetic conditions, Müller cells become reactivated, as demonstrated by the increase of intermediate filament proteins (e.g., glial fibrillary acidic protein, vimentin[44,62]). Continuous reactivation or reactive gliosis induces functional and structural changes, such as decreased and increased expression of Kir4.1- and AQP4-positive channels, respectively, and subcellular mislocalization, leading to uncoupling of AQP4 from Kir4.1.[22,63] These changes lead to reduced potassium efflux and increased water retention, inducing swelling of the Müller cells and retinal thickening. Another potential role for AQP4 is its function in the "glymphatic" system, which might be involved in protein and fluid drainage from the retina.[61,64] Although the link between PKal and the reactivation of Müller cells or disruption of Kir4.1 and AQP4 in the retina has not been investigated, inhibition of Kir4.1 by bradykinin has been described in the kidney.[65] Our study is the first, to our knowledge, demonstrating that inhibition of PKal can reduce the process of reactive gliosis by restoring the decreased expression of Kir4.1-positive potassium channels in the diabetic retina, potentially leading to reduced vascular leakage and retinal thickening. Although the mislocalization of the potassium channels at the Müller glial endfeet around the vessels was not specifically investigated here, this overall Kir4.1 reduction may be an important finding regarding the mechanism how THR-149 can prevent diabetes-induced retinal changes.

Based on the results of the current study, PKal seems to be an important mediator in diabetes-induced BRB dysfunction and thickening of retinal layers. As such, exploration of the potential of THR-149 in a clinical setting seems to be a logical next step. A phase 1 open-label, multicenter trial evaluated the safety of a single IVT injection of THR-149 at three ascending dose levels in 12 subjects with visual impairment due to center-involved DME. Data from this trial showed that THR-149 was well tolerated and safe. No dose-limiting toxicities nor drug-related serious adverse events were

reported at any of the dosages evaluated in the study. Central subfield thickness changes were within the variability of measurement, in line with the results reported in this study following the administration of a single injection. A rapid onset of action in best-corrected visual acuity (BCVA) was observed from day 1, with an increasing average improvement of up to 7.5 letters on day 14. This activity was maintained with an average improvement in BCVA of 6.5 letters on day 90 following a single injection of THR-149 (Dugel et al.[69]). Interestingly, increased expression of vitreous inflammatory cytokines might correlate with worse BCVA in diabetic patients,[66] and a rapid improvement on BCVA can potentially be linked to decreased retinal inflammation.[67] As such, this may potentially explain the BCVA improvement after a single injection of THR-149 in the phase 1 study, as an anti-inflammatory effect in the current diabetic rat STZ study was also observed after a single IVT injection at 4 weeks post-diabetes onset.

Taken together, these results further demonstrate the role of PKal in DME, suggesting that this pathway is linked to many processes relating to leakage and fluid homeostasis in the retina, and support the development of THR-149 as a treatment option for this ocular disease. Although a single injection of THR-149 induced an anti-inflammatory effect, here we showed, that repeated administration of the PKal inhibitor reduces activation of retinal microglia/macrophages, retinal levels of IL-6, vascular leakage, and retinal thickening via decreasing Müller cell activation and by restoring the reduced Kir4.1-positive channels in the diabetic retina. As such, our findings potentially indicate that repeated IVT injections are needed to induce its complete therapeutic effect.

Acknowledgments

The authors thank Astrid De Vriese, Bernard Noppen, Huberte Moreau, Isabelle Etienne, Nele Leenders, Lies Rousel, Luca Masin, Sandra Jansen, Sofie Molenberghs, and Valerie Vanheukelom for their technical support.

Disclosure: **T. Van Bergen**, Oxurion NV (F); **T.-T. Hu**, Oxurion NV (F); **K. Little**, None; **L. De Groef**, None; **L. Moons**, None; **A. W. Stitt**, Oxurion NV (F); **E. Vermassen**, Oxurion NV (F); **J.H.M. Feyen**, Oxurion NV (F)

References

1. Lee R, Wong TY, Sabanayagam C. Epidemiology of diabetic retinopathy, diabetic macular edema and related vision loss. *Eye Vis (Lond)*. 2015;2:17.
2. Rivera JC, Dabouz R, Noueihed B, Omri S, Tahiri H, Chemtob S. Ischemic retinopathies: oxidative stress and inflammation. *Oxid Med Cell Longev*. 2017;2017:3940241.
3. Stitt AW, Curtis TM, Chen M, et al. The progress in understanding and treatment of diabetic retinopathy. *Prog Retin Eye Res*. 2016;51:156–186.
4. Duh EJ, Sun JK, Stitt AW. Diabetic retinopathy: current understanding, mechanisms, and treatment strategies. *JCI Insight*. 2017;2:e93751.
5. Bressler SB, Qin H, Beck RW, et al. Factors associated with changes in visual acuity and central subfield thickness at 1 year after treatment for diabetic macular edema with ranibizumab. *Arch Ophthalmol*. 2012;130:1153–1161.
6. Bressler SB, Odia I, Maguire MG, et al. Factors associated with visual acuity and central subfield thickness changes when treating diabetic macular edema with anti-vascular endothelial growth factor therapy: an exploratory analysis of the Protocol T randomized clinical trial. *JAMA Ophthalmol*. 2019;137:382–389.
7. Feener EP. Plasma kallikrein and diabetic macular edema. *Curr Diab Rep*. 2010;10:270–275.
8. Liu J, Feener EP. Plasma kallikrein-kinin system and diabetic retinopathy. *Biol Chem*. 2013;394:319–328.
9. Bhatwadekar AD, Kansara VS, Ciulla TA. Investigational plasma kallikrein inhibitors for the treatment of diabetic macular edema: an expert assessment. *Expert Opin Investig Drugs*. 2020;29:237–244.
10. Abdouh M, Talbot S, Couture R, Hassessian HM. Retinal plasma extravasation in streptozotocin-diabetic rats mediated by kinin B(1) and B(2) receptors. *Br J Pharmacol*. 2008;154:136–143.
11. Gao BB, Clermont A, Rook S, et al. Extracellular carbonic anhydrase mediates hemorrhagic retinal and cerebral vascular permeability through prekallikrein activation. *Nat Med*. 2007;13:181–188.
12. Kita T, Clermont AC, Murugesan N, et al. Plasma kallikrein-kinin system as a VEGF-independent mediator of diabetic macular edema. *Diabetes*. 2015;64:3588–3599.
13. Gao BB, Chen X, Timothy N, Aiello LP, Feener EP. Characterization of the vitreous proteome in diabetes without diabetic retinopathy and diabetes with proliferative diabetic retinopathy. *J Proteome Res*. 2008;7:2516–2525.
14. Brondani LA, Crispim D, Pisco J, Guimaraes JA, Berger M. The G allele of the rs12050217 polymorphism in the BDKRB1 gene is associated with protection for diabetic retinopathy. *Curr Eye Res*. 2019;44:994–999.
15. Clermont A, Chilcote TJ, Kita T, et al. Plasma kallikrein mediates retinal vascular dysfunction and induces retinal thickening in diabetic rats. *Diabetes*. 2011;60:1590–1598.
16. Murugesan N, Fickweiler W, Clermont AC, Zhou Q, Feener EP. Retinal proteome associated with bradykinin-induced edema. *Exp Eye Res*. 2019;186:107744.
17. Clermont A, Murugesan N, Zhou Q, et al. Plasma kallikrein mediates vascular endothelial growth factor-induced retinal dysfunction and thickening. *Invest Ophthalmol Vis Sci*. 2016;57:2390–2399.
18. Catanzaro O, Labal E, Andornino A, Capponi JA, Di Martino I, Sirois P. Blockade of early and late retinal biochemical alterations associated with diabetes development by the selective bradykinin B1 receptor antagonist R-954. *Peptides*. 2012;34:349–352.
19. Lawson SR, Gabra BH, Nantel F, Battistini B, Sirois P. Effects of a selective bradykinin B1 receptor antagonist on increased plasma extravasation in streptozotocin-induced diabetic rats: distinct vasculopathic profile of major key organs. *Eur J Pharmacol*. 2005;514:69–78.
20. Pouliot M, Talbot S, Senecal J, Dotigny F, Vaucher E, Couture R. Ocular application of the kinin B1 receptor antagonist LF22-0542 inhibits retinal inflammation and oxidative stress in streptozotocin-diabetic rats. *PLoS One*. 2012;7:e33864.
21. Teufel DP, Bennett G, Harrison H, et al. Stable and long-lasting, novel bicyclic peptide plasma kallikrein inhibitors for the treatment of diabetic macular edema. *J Med Chem*. 2018;61:2823–2836.
22. Zhang Y, Xu G, Ling Q, Da C. Expression of aquaporin 4 and Kir4.1 in diabetic rat retina: treatment with minocycline. *J Int Med Res*. 2011;39:464–479.
23. Qaum T, Xu Q, Joussen AM, et al. VEGF-initiated blood-retinal barrier breakdown in early diabetes. *Invest Ophthalmol Vis Sci*. 2001;42:2408–2413.
24. Davis EJ, Foster TD, Thomas WE. Cellular forms and functions of brain microglia. *Brain Res Bull*. 1994;34:73–78.
25. Raibon E, Sauve Y, Carter DA, Gaillard F. Microglial changes accompanying the promotion of retinal ganglion cell axonal

regeneration into peripheral nerve grafts. *J Neurocytol*. 2002;31:57–71.
26. Noailles A, Fernandez-Sanchez L, Lax P, Cuenca N. Microglia activation in a model of retinal degeneration and TUDCA neuroprotective effects. *J Neuroinflammation*. 2014;11:186.
27. Van Bergen T, Hu T-T, Etienne I, Reyns GE, Moons L, Feyen JHM. Neutralization of placental growth factor as a novel treatment option in diabetic retinopathy. *Exp Eye Res*. 2017;165:136–150.
28. Davis BM, Salinas-Navarro M, Cordeiro MF, Moons L, De GL. Characterizing microglia activation: a spatial statistics approach to maximize information extraction. *Sci Rep*. 2017;7:1576.
29. Jurga AM, Paleczna M, Kuter KZ. Overview of general and discriminating markers of differential microglia phenotypes. *Front Cell Neurosci*. 2020;14:198.
30. Vila GM, Eleftheriadou M, Kelaini S, et al. Endothelial cells derived from patients with diabetic macular edema recapitulate clinical evaluations of anti-VEGF responsiveness through the neuronal pentraxin 2 pathway. *Diabetes*. 2020;69:2170–2185.
31. Lim SW, Bandala-Sanchez E, Kolic M, et al. The influence of intravitreal ranibizumab on inflammation-associated cytokine concentrations in eyes with diabetic macular edema. *Invest Ophthalmol Vis Sci*. 2018;59:5382–5390.
32. Sohn HJ, Han DH, Kim IT, et al. Changes in aqueous concentrations of various cytokines after intravitreal triamcinolone versus bevacizumab for diabetic macular edema. *Am J Ophthalmol*. 2011;152:686–694.
33. Lai AKW, Lo ACY. Animal models of diabetic retinopathy: summary and comparison. *J Diabetes Res*. 2013;2013:106594.
34. Canning P, Kenny BA, Prise V, et al. Lipoprotein-associated phospholipase A2 (Lp-PLA2) as a therapeutic target to prevent retinal vasopermeability during diabetes. *Proc Natl Acad Sci USA*. 2016;113:7213–7218.
35. Zhang X, Bao S, Lai D, Rapkins RW, Gillies MC. Intravitreal triamcinolone acetonide inhibits breakdown of the blood-retinal barrier through differential regulation of VEGF-A and its receptors in early diabetic rat retinas. *Diabetes*. 2008;57:1026–1033.
36. Desjardins DM, Yates PW, Dahrouj M, Liu Y, Crosson CE, Ablonczy Z. Progressive early breakdown of retinal pigment epithelium function in hyperglycemic rats. *Invest Ophthalmol Vis Sci*. 2016;57:2706–2713.
37. Barber AJ, Lieth E, Khin SA, Antonetti DA, Buchanan AG, Gardner TW. Neural apoptosis in the retina during experimental and human diabetes. Early onset and effect of insulin. *J Clin Invest*. 1998;102:783–791.
38. Park SH, Park JW, Park SJ, et al. Apoptotic death of photoreceptors in the streptozotocin-induced diabetic rat retina. *Diabetologia*. 2003;46:1260–1268.
39. Kiyosawa I. Age-related changes in visual function and visual organs of rats. *Exp Anim*. 1996;45:103–114.
40. Goebel W, Kretzchmar-Gross T. Retinal thickness in diabetic retinopathy: a study using optical coherence tomography (OCT). *Retina*. 2002;22:759–767.
41. Huber G, Heynen S, Imsand C, et al. Novel rodent models for macular research. *PLoS One*. 2010;5:e13403.
42. Short BG. Safety evaluation of ocular drug delivery formulations: techniques and practical considerations. *Toxicol Pathol*. 2008;36:49–62.
43. Del Amo EM, Rimpela AK, Heikkinen E, et al. Pharmacokinetic aspects of retinal drug delivery. *Prog Retin Eye Res*. 2017;57:134–185.
44. Rungger-Brandle E, Dosso AA, Leuenberger PM. Glial reactivity, an early feature of diabetic retinopathy. *Invest Ophthalmol Vis Sci*. 2000;41:1971–1980.
45. Ascaso FJ, Huerva V, Grzybowski A. The role of inflammation in the pathogenesis of macular edema secondary to retinal vascular diseases. *Mediators Inflamm*. 2014;2014:432685.
46. Chung YR, Kim YH, Ha SJ, et al. Role of inflammation in classification of diabetic macular edema by optical coherence tomography. *J Diabetes Res*. 2019;2019:8164250.
47. Dong N, Xu B, Chu L, Tang X. Study of 27 aqueous humor cytokines in type 2 diabetic patients with or without macular edema. *PLoS One*. 2015;10:e0125329.
48. Funatsu H, Yamashita H, Noma H, Mimura T, Yamashita T, Hori S. Increased levels of vascular endothelial growth factor and interleukin-6 in the aqueous humor of diabetics with macular edema. *Am J Ophthalmol*. 2002;133:70–77.
49. Funatsu H, Noma H, Mimura T, Eguchi S, Hori S. Association of vitreous inflammatory factors with diabetic macular edema. *Ophthalmology*. 2009;116:73–79.
50. Kumar B, Gupta SK, Nag TC, et al. Retinal neuroprotective effects of quercetin in streptozotocin-induced diabetic rats. *Exp Eye Res*. 2014;125:193–202.
51. Kern TS. Contributions of inflammatory processes to the development of the early stages of diabetic retinopathy. *Exp Diabetes Res*. 2007;2007:95103.
52. Yao Y, Li R, Du J, Long L, Li X, Luo N. Interleukin-6 and diabetic retinopathy: a systematic review and meta-analysis. *Curr Eye Res*. 2019;44:564–574.
53. Zhou X, Polgar P, Taylor L. Roles for interleukin-1beta, phorbol ester and a post-transcriptional regulator in the control of bradykinin B1 receptor gene expression. *Biochem J*. 1998;330(pt 1):361–366.
54. Couture R, Blaes N, Girolami JP. Kinin receptors in vascular biology and pathology. *Curr Vasc Pharmacol*. 2014;12:223–248.
55. Leeb-Lundberg LM, Marceau F, Muller-Esterl W, Pettibone DJ, Zuraw BL. International union of pharmacology. XLV. Classification of the kinin receptor family: from molecular mechanisms to pathophysiological consequences. *Pharmacol Rev*. 2005;57:27–77.
56. Schwaninger M, Sallmann S, Petersen N, et al. Bradykinin induces interleukin-6 expression in astrocytes through activation of nuclear factor-kappaB. *J Neurochem*. 1999;73:1461–1466.
57. Hachana S, Fontaine O, Sapieha P, Lesk M, Couture R, Vaucher E. The effects of anti-VEGF and kinin B1 receptor blockade on retinal inflammation in laser-induced choroidal neovascularization. *Br J Pharmacol*. 2020;177:1949–1966.
58. Huang CD, Tliba O, Panettieri RA, Jr, Amrani Y. Bradykinin induces interleukin-6 production in human airway smooth muscle cells: modulation by Th2 cytokines and dexamethasone. *Am J Respir Cell Mol Biol*. 2003;28:330–338.
59. Terzuoli E, Meini S, Cucchi P, et al. Antagonism of bradykinin B2 receptor prevents inflammatory responses in human endothelial cells by quenching the NF-κB pathway activation. *PLoS One*. 2014;9:e84358.
60. Reichenbach A, Bringmann A. New functions of Müller cells. *Glia*. 2013;61:651–678.
61. Daruich A, Matet A, Moulin A, et al. Mechanisms of macular edema: beyond the surface. *Prog Retin Eye Res*. 2018;63:20–68.
62. Lewis GP, Fisher SK. Up-regulation of glial fibrillary acidic protein in response to retinal injury: its potential role in glial remodeling and a comparison to vimentin expression. *Int Rev Cytol*. 2003;230:263–290.
63. Reichenbach A, Wurm A, Pannicke T, Iandiev I, Wiedemann P, Bringmann A. Müller cells as players in retinal degeneration and edema. *Graefes Arch Clin Exp Ophthalmol*. 2007;245:627–636.

Investigative Ophthalmology & Visual Science

64. Wang X, Lou N, Eberhardt A, et al. An ocular glymphatic clearance system removes β-amyloid from the rodent eye. *Sci Transl Med*. 2020;12:eaaw3210.
65. Zhang DD, Gao ZX, Vio CP, et al. Bradykinin stimulates renal Na(+) and K(+) excretion by inhibiting the K(+) channel (Kir4.1) in the distal convoluted tubule. *Hypertension*. 2018;72:361–369.
66. Petrovic MG, Korosec P, Kosnik M, Hawlina M. Association of preoperative vitreous IL-8 and VEGF levels with visual acuity after vitrectomy in proliferative diabetic retinopathy. *Acta Ophthalmol*. 2010;88:e311–e316.
67. Veritti D, Sarao V, Galiazzo F, Lanzetta P. Early effects of dexamethasone implant on macular morphology and visual function in patients with diabetic macular edema. *Ophthalmologica*. 2017;238:100–105.
68. Van Bergen T, Hu TT, Etienne I, Feyen JHM. Targeting plasma kallikrein with a novel bicyclic peptide inhibitor reduced retinal leakage in a diabetic rat model. *Proceedings of the 28th Meeting of the European Association for the Study of Diabetes Eye Complications Study Group (EASDec): Belfast, Northern Ireland*. 2018.
69. Dugel PU, Khanani A, Berger B, Patel S, Fineman MS, Jaffe GJ, Kozma-Wiebe P, Heier JS. Phase 1 dose-escalation study of plasma kallikrein inhibitor THR-149 for the treatment of diabetic macular edema. *Transl Vis Sci Technol*. (accepted).

Investigative Ophthalmology & Visual Science